

## The role of dunes in flow resistance in a large and a small river. The case of the Paraná and Tercero rivers, Argentina

Francisco G. Latosinski, Mario L. Amsler, Carlos A. Vionnet, Ana I. Heredia Ligorria, Ricardo N. Szupiany, José M. Diaz Lozada, Carlos M. García & Marcelo H. García

To cite this article: Francisco G. Latosinski, Mario L. Amsler, Carlos A. Vionnet, Ana I. Heredia Ligorria, Ricardo N. Szupiany, José M. Diaz Lozada, Carlos M. García & Marcelo H. García (2022): The role of dunes in flow resistance in a large and a small river. The case of the Paraná and Tercero rivers, Argentina, Journal of Hydraulic Research, DOI: [10.1080/00221686.2021.2001588](https://doi.org/10.1080/00221686.2021.2001588)

To link to this article: <https://doi.org/10.1080/00221686.2021.2001588>



Published online: 10 Jan 2022.



Submit your article to this journal [↗](#)



View related articles [↗](#)



View Crossmark data [↗](#)



Research paper

## The role of dunes in flow resistance in a large and a small river. The case of the Paraná and Tercero rivers, Argentina

FRANCISCO G. LATOSINSKI, Researcher, Assistant Professor, *National Council for Scientific and Technological Research (CONICET), Universidad Nacional del Litoral, CC 217, CP 3000, Santa Fe, Argentina*  
Email: [flatosinski@fich.unl.edu.ar](mailto:flatosinski@fich.unl.edu.ar) (author for correspondence)

MARIO L. AMSLER, Researcher, Professor, *National Institute of Limnology (INALI-CONICET), Universidad Nacional del Litoral, Ciudad Universitaria, CP 3000, Santa Fe, Argentina*  
Email: [mamsler2003@yahoo.com.ar](mailto:mamsler2003@yahoo.com.ar)

CARLOS A. VIONNET, Researcher, Professor, *National Council for Scientific and Technological Research (CONICET), Universidad Nacional del Litoral, CC 217, CP 3000, Santa Fe, Argentina*  
Email: [carlos.vionnet@gmail.com](mailto:carlos.vionnet@gmail.com)

ANA I. HEREDIA LIGORRIA, PhD Student, Assistant Professor, *National Council for Scientific and Technological Research (CONICET), Universidad Nacional de Córdoba, Av. Filloy s/n, Ciudad Universitaria, Córdoba, Argentina*  
Email: [ana.heredia@unc.edu.ar](mailto:ana.heredia@unc.edu.ar)

RICARDO N. SZUPIANY, Researcher, Professor, *National Council for Scientific and Technological Research (CONICET), Universidad Nacional del Litoral, CC 217, CP 3000, Santa Fe, Argentina*  
Email: [rszupian@fich.unl.edu.ar](mailto:rszupian@fich.unl.edu.ar)

JOSÉ M. DIAZ LOZADA, Assistant Professor, *National Council for Scientific and Technological Research (CONICET), Universidad Nacional de Córdoba, Av. Filloy s/n, Ciudad Universitaria, Córdoba, Argentina*  
Email: [jmdiazlozada@gmail.com](mailto:jmdiazlozada@gmail.com)

CARLOS M. GARCÍA, Researcher, Professor, *National Council for Scientific and Technological Research (CONICET), Universidad Nacional de Córdoba, Av. Filloy s/n, Ciudad Universitaria, Córdoba, Argentina*  
Email: [cgarcia2mjc@gmail.com](mailto:cgarcia2mjc@gmail.com)

MARCELO H. GARCÍA  (IAHR Member), M.T. Geoffrey Yeh Chair, Professor and Director, *Ven Te Chow Hydrosystems Laboratory, Department of Civil and Environmental Eng., University of Illinois at Urbana-Champaign, 205 N. Matthews, Urbana, Illinois, 61801, USA*  
Email: [mhgarcia@illinois.edu](mailto:mhgarcia@illinois.edu)

### ABSTRACT

The dynamics of sandy rivers is a complex phenomenon linking the interactions between dunes, flow and sediment transport. Despite an existing large amount of research, few comparative studies exist for rivers with major hydro-sedimentological differences. This work uses detailed dune measurements from the Paraná and Tercero rivers, Argentina. Significant differences were found in the representative roughness height scale, dune steepness, lee angles, velocity profiles and flow recirculation. It is found that whereas the hydraulic resistance for the Tercero River scales with the size of large dunes, the Paraná River needs to develop an intermediate roughness scale (the small superimposed dunes) to accommodate the required balance between gravity and friction. Suspended bed sediment increase is inversely related to the dune steepness and lee side angles as advanced by previous findings. The suspension number seems to be a paramount metric that helps explain differences regarding dune geometry within a wide range of flow conditions.

**Keywords:** Bedload; field measurements; flow resistance; Paraná and Tercero rivers; river dunes; suspended bed sediments

Received 1 December 2019; accepted 29 September 2021/Currently open for discussion.

## 1 Introduction

Bedforms are known to interact with the stream to modify the flow resistance, bed morphology and sediment transport in natural erodible channels. In sand-bedded rivers, flow resistance is usually partitioned between grain and form resistance. However, the physical processes implied in these interactions remain to be fully elucidated (Best, 2005; Bradley & Venditti, 2017; Cisneros et al., 2020).

The research literature on lab-based studies (Bradley & Venditti, 2019; Kwoil et al., 2016; McLean, Wolfe, & Nelson, 1999; Nelson, McLean, & Wolfe, 1993; Van Rijn, 1993; Yalin & Karahan, 1979; among many others), along with field measurements (Amsler & Prendes, 2000; Kostaschuk et al., 2009; Parsons et al., 2005; Shugar et al., 2010; Smith & McLean, 1977; Trento, Amsler, & Pujol, 1990), and numerical modelling (Lefebvre, 2019; Lefebvre & Winter, 2016; Schmeeckle et al., 1999; Tjerry & Fredsøe, 2005) have made a significant contribution to the subject. Most early research focuses on certain similarities in flow characteristics at river and laboratory scales. The salient dunes features obtained from these studies were: flow separation downstream of the dune crest, an abrupt lee face with an angle close to the repose of sands and flow reattachment on the stoss side of the downstream dune (Best, 2005; Holmes & García, 2008).

The review by Best (2005) remarked that the classical model of flow over dunes was not in line with the results of observations, basically of dunes in low-gradient rivers. However, many researchers recognized that bedforms in large sand-bedded rivers and coastal environments are characterized with slip face slopes lower than the angle-of-repose, the so-called low-angle bedforms (Best, 2005; Lefebvre, 2019). Over such bedforms, no permanent flow separation is observed (Best, 2005). Indeed, bedforms studied in laboratory flumes generally develop steeper slip faces than bedforms found in natural channels (Naqshband, Ribberink, & Hulscher, 2014). Recent investigations that deviated from the classical scheme showed that natural dunes with low lee-angles and different shapes have various implications for the flow and shear stress mechanics (Cisneros et al., 2020; Lefebvre & Winter, 2016; Lefebvre, Paarlberg, & Winter, 2016).

Over the last 15 years, investigations based on modern technologies of field measurements have contributed to significant advances to the classical model criticized by Best (2005), through the observation of flow over natural dunes. Parsons et al. (2005) studied the influence of bedform three-dimensionality on the 3D flow structure at an upper reach of the Paraná River main channel. They found that the flow separation zone is closely associated with the lee-side angle, extended over an extremely narrow area of the channel bed, and concluded that the flow structure of a three-dimensional bed is related to smaller levels of large-scale turbulence than its two-dimensional counterpart. Thus, suspended bed sediment may be lower and sediment transport over the dune field may be reduced. Kostaschuk et al. (2009) found, upstream of the

confluence of the Paraguay-Paraná Rivers, that suspended bed sediment concentrations are higher over the crest of a dune in comparison to its trough. These authors reported that nearly 17% of the suspended sediments were being deposited over the lee face of the dune, and argue that deposition governed its steepness and contributed to the dune displacement. However, bed load was not part of their analysis. Other studies, also in the Paraná River, have reported strong and negative correlations between streamwise velocity and the vertical velocity over a dune crest (Shugar et al., 2010). On the other hand, the observed positive correlation between vertical velocity/suspended bed sediment concentration and the reverse for streamwise velocity/suspended bed sediment concentration were associated with the sediment supply from the bed to the layers of adjacent flow (Shugar et al., 2010).

An important issue related to flow over dunes is the separation zone downstream of alluvial dunes, which has been long recognized as one of the main sources of energy losses and resistance to flow in alluvial streams, the so-called “form” resistance (e.g. Kennedy, 1975). Later on, based on measurements conducted in laboratories and natural dunes, the effective existence of flow separation and recirculation behind crests of natural dunes and their influence on flow resistance as the key factor was questioned (c.f. Amsler & Schreider, 1992; Kostaschuk, 2000; Lefebvre, 2019; Ogink, 1989; Parsons et al., 2005). The intermittency of flow separation along lee sides of low-angle dunes would reduce the importance of form drag (compared to steeper dunes) on the overall flow resistance in large rivers, where low-angle dunes are commonly observed (Amsler & Schreider, 1992; Amsler & Prendes, 2000; Bradley & Venditti, 2017; Cisneros et al., 2020; Naqshband et al., 2014; Ogink, 1989). Indeed, the existence of a brink-point in the lee side of the natural dunes with maximum lee angles  $< 10^\circ$  verifies its occurrences at the lower depths of the lee-side without permanent flow separation (Cisneros et al., 2020). For lee-side angles greater than  $\sim 15\text{-}20^\circ$ , the presence and size of flow separation are determined by the height of the brink-point rather than by the dune height (Lefebvre, 2019) and by the orientation of the slipface (the portion of the lee side with angles  $> 15^\circ$ ) compared to the mean flow. Regarding the intermediate maximum angles ( $\sim 10\text{-}18^\circ$ ), flow separation could be intermittent (Cisneros et al., 2020). In an effort to discriminate large (generally with lower lee angles) from small (generally with larger lee angles) dunes, Bradley and Venditti (2017) found a break in the scaling relation that occurs at a water depth of 2.5 m that allows determination of the dominant process that controls the dune dimensions.

At least two important questions related to bed roughness height and the resistance to flow arise: (i) is there any relation between the hydraulic resistance with the lee-side angles and the dominant sediment transport modes? and (ii) is it possible to discriminate the differences implied in (i) through a simple scale parameter based on the mean flow structure and bed sediment texture? While these questions are partially addressed by

different authors, detailed field investigations comparing dune dynamics in rivers with quite different characteristics remain to be done.

Bradley and Venditti (2017) offered a compilation of flow and dune dimension data to evaluate the scaling relations of dunes. Here, the proposed scaling is based on the classical wall-similarity approach. This paper deals with the question of whether similarity profiles of dunes and flow occur on sandy bed rivers by presenting detailed measurements of dune geometry, flow structure, and sediment transport (suspended as well as bed load) along with dune profiles in two rivers with substantially different discharges and bed sediment textures, the Paraná and Tercero rivers in Argentina.

The Paraná River is a medium sand bed river with a nearly uniform (well-sorted) bed sediment distribution, with an average diameter of around 350  $\mu\text{m}$ . The Tercero River is a very coarse sand bed river with a poorly-sorted distribution according to conventional classifications, with average sizes of the order of 1.95 mm.

The purpose of this study is twofold. Firstly, it aims at partially answering the two questions stated above by identifying the relevant scaling parameters for dunes in a large and a small river. Secondly, it seeks to establish the disparities in the length scales that characterize the hydraulic resistance in both rivers.

The following sections show that despite both rivers having bedform shape similarity there is a significant difference in the characteristic height for the hydraulic resistance and the predominant mode of sediment transport between them. Both rivers obey Keulegan's resistance law within the bounds of the normal flow approximation, which assumes a perfect balance between friction and gravity (Keulegan, 1938). Nevertheless, it is found that whereas the hydraulic resistance for the Tercero River scales with the dune sizes, the Paraná River needs to develop an intermediate roughness scale to accommodate the required balance between gravity and friction. This in-between length scale fits the size of small dunes found superimposed on the large dunes of the Paraná River. Finally, it is corroborated that the suspension number is an adequate parameter to account for the variations of the lee-side angles of dunes.

## 2 Field sites and methodology

### 2.1 Field sites

Bedforms were analysed in a large river (Paraná River, Argentina) and a small river (Tercero River, also known as Citalamochita River, Argentina). Four river reaches were surveyed, the first one is located in the Tercero River and the other three are located in the main channel of the Paraná River (Fig. 1). The main geometric, hydraulic, and sedimentologic features from both rivers are summarized in Table 1. From data in Table 1, large differences emerge not only in water discharges, mean depths or sediment transport, but also in the bed sediment size

as mentioned previously. Indeed, the Tercero River has medium bottom particle sizes and Reynolds particle numbers, nearly 6 and 13 times larger than the Paraná River's, respectively (Tables 2 and 3).

Tercero River measurements were performed at Villa María city, 120 km downstream from Almafuerite city where the Piedras Moras Dam regulates the discharges, from Alberdi bridge (32°25'19''S, 63°14'23''W; Fig. 1a) during four measurement campaigns in 2016 (Table 2). Longitudinal bathymetric records, flow velocity, discharge and bed-particle velocity were recorded using a YSI/SonTek 3000 kHz ADCP (S5) linked to a DGPS using the VTG reference technique (horizontal position accuracy less than 1 m at approximately 2 Hz). This section is located at a straight reach with expected quasi-2D bedforms and the measurements were taken under quite steady flow conditions.

Measurements in the Paraná River were performed at three reaches (Table 2): Lavalle (29°0'60''S, 59°12'5''W, Fig. 1b), Aguas Corrientes (31°41'21''S, 60°28'3''W, Fig. 1c) and Bajada Grande (31°44'13''S, 60°39'43''W, Fig. 1d). A 1200 kHz Teledyne RDI Rio Grande ADCP was connected to a DGPS with RTK corrections (position accuracy of  $\pm 0.03$  m at approximately 1 Hz). Depths were obtained by means of a 200 Hz Raytheon single-beam echo-sounder (SBES) linked to the RTK-DGPS. All the equipment was deployed on a survey boat. These reaches were selected according to the different morphological features of the multi-thread pattern of the Paraná River, such as straight reaches (Lavalle), narrowing sections (Aguas Corrientes), and along a bifurcated branch of upstream multiple bifurcations (Bajada Grande). All measurements were surveyed along the thalweg of the main channel.

The hydrographs of daily levels during 2011 and 2012 at two gauge stations (Empedrado, near Lavalle, and Paraná Port, 2 km downstream Aguas Corrientes), are shown in Fig. 2. The dates of field surveys in the Paraná River are also included in the figure. As it is typical in large and very large streams the variations of levels are normally very gradual. Thus, lag effects producing changes in dune dimensions were not expected. Nevertheless, Amsler and García (1997; see also García, 2008, figure 2-46) recorded a certain lag in the accommodation of large dune dimensions after a moderate flood in the Paraná River. Given this evidence, the dune steepness recorded at Lavalle (Fig. 2) might be expected to be smaller than those corresponding to mean water stages. Tercero River does not have an automatic gauging station in the study zone; thus, water stages were roughly inferred from measured water discharge at fieldworks (Table 2). However, owing to the fact that the Tercero River discharge at the field site is regulated by the upstream Piedras Moras Dam, and to the lack of significant discharge contribution between the dam and Villa Maria city, each measurement was performed after one or two weeks of constant discharge in arrangement with the dam-management staff. Taking into account the turnover time (Myrow et al. 2018) of a couple of hours for the Tercero River, obtained from mean

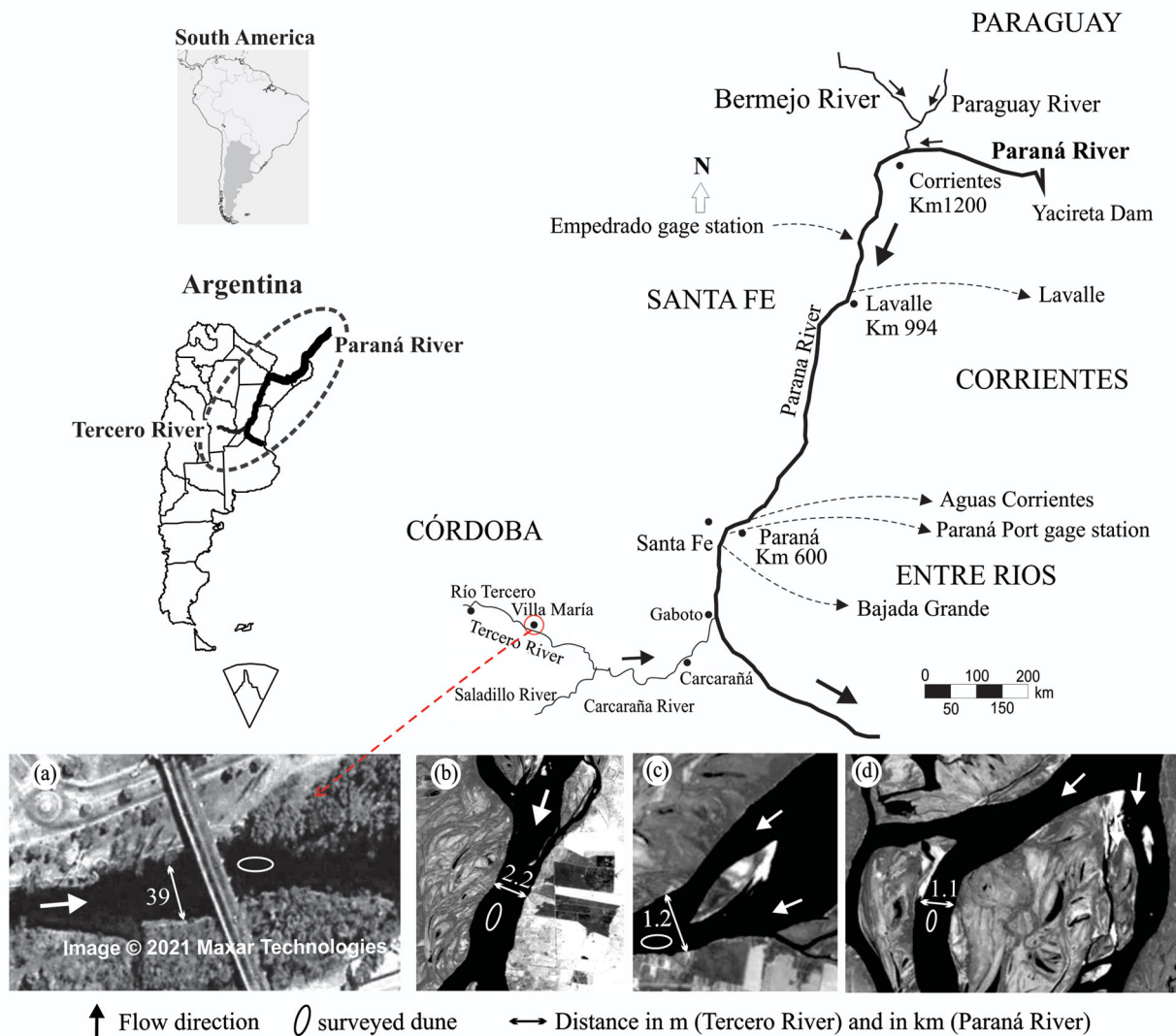


Figure 1 Location of river reaches surveyed in the study: (a) Tercero River near Villa María city (Córdoba); and Paraná River in (b) Lavalle (Corrientes), (c) Aguas Corrientes (Entre Ríos) and (d) Bajada Grande (Entre Ríos)

Table 1 Main average parameters of Tercero and Paraná Rivers

River	$Q$ ( $m^3 s^{-1}$ )	$B$ (m)	$H$ (m)	$U$ ( $m s^{-1}$ )	$S$	$D_{50}$ (mm)	$\sigma_g$	Sediment transport ( $ton year^{-1}$ )		
								$G_w$	$G_{sf}$	$G_{sb}$
Tercero	27	30–42	1	0.9	$0.56 \times 10^{-03}$ *	1.95	1.96	**	**	**
Paraná	19,500	600–2,500	10	1.2	$\sim 10^{-05}$	0.35	1.52	$9.42 \times 10^7$	$2.2 \times 10^6$	$2.32 \times 10^7$

Variables in the table:  $B$  width;  $h$  depth;  $Q$  discharge;  $u$  flow velocity;  $S$  surface slope;  $D_{50}$  median grain size of bed sediment;  $\sigma_g$  geometric standard deviation;  $G_w$ ,  $G_{sf}$ , and  $G_{sb}$  annual sediment transport of washload, suspended bed-sediment, and bedload,  $G_{sb}$ , respectively.

\*General slopes values of the alluvial plain (without data of water surface slopes, from Riccardi et al., 2013). However, water surface slope measured 170 km downstream the study site with an RTK-DGPS by Herrero et al. (2018) was  $0.18 \times 10^{-3}$ .

\*\*Without systematic data.

bedform features, one and two weeks of constant discharge is a reasonable time.

## 2.2 Methodology

Moving and fixed boat ADCP measurements were used in both rivers at each fieldwork. Dynamic measurements in the Paraná

River were performed along two longitudinal profiles 1.5 km long over a sequence of dunes, from downstream to upstream. Each track was surveyed at the beginning and end of each day ( $\sim 7$  h interval time) to capture an appreciable dune displacement. The successive records of a selected dune were used to estimate the bedload rate by means of the dune tracking method (Simons, Richardson, & Nordin, 1965), and to record

Table 2 Bedform, flow and sediment features along the study dunes in the Tercero and Paraná Rivers. Values of  $h$  and  $u$  were spatially averaged along dunes on the thalweg

Site and date	$Q$ ( $m^3 s^{-1}$ )	$F_r$	$\lambda_d$ (m)	$H_d$ (m)	$H_d/\lambda_d$	$B^i$ (degrees)	$\alpha$	$D_{50}$ (mm)	$\sigma_g$	$h$ (m)	$H_d/h$	$B$ (m)	$u$ ( $m s^{-1}$ )
TR 16 Mar 2016	114	0.29	4.5	0.40	0.09	25–12	0.64	1.95	1.96	2.5	0.16	39	1.45
TR 8 Apr 2016	66	0.31	6.1	0.48	0.08	36–16	0.47	1.95	1.96	1.5	0.32	33	1.21
TR 5 Sep 2016	25	0.21	1.9	0.20	0.10	22–13	0.54	1.95	1.96	1.1	0.18	32	0.70
TR 7 Nov 2016	19	0.28	2.2	0.24	0.11	38–29	0.75	1.95	1.96	1.1	0.22	32	0.92
Lavalle 2 Jun 2011	17100	0.11	185.3	1.93	0.01	14–3	0.78	0.31	1.52	8.7	0.22	2250	1.04
AC 26 Apr 2012	12500	0.10	134.3	2.86	0.02	15–5	0.58	0.34	1.48	18.2	0.16	1200	1.36
BG 26 Jul 2012	8900 <sup>ii</sup>	0.12	138.7	1.78	0.01	6–2	0.68	0.39	1.55	9.4	0.19	1100	1.17

Variables in the table:  $\lambda_d$  length;  $H_d$  height;  $H_d/\lambda_d$  steepness;  $\beta$  lee-side angle;  $H_d/h$  relative height;  $\alpha$  form factor which accounts for deviations of bed-form shape from an idealized triangle

Note: TR: Tercero River, AC: Aguas Corrientes, BG: Bajada Grande

<sup>i</sup>Maximum and average values for the lee-side angle (Fig. 5)

<sup>ii</sup>Measurements performed at the principal branch of the main channel. The Paraná River divides into several branches immediately upstream of the Bajada Grande site measurement. Total discharge at BG 26 Jul 2012:  $16,000 m^3 s^{-1}$ .

The steepness of superimposed dunes observed in the Paraná River were 0.04, 0.07 and 0.04 for Lavalle 2 Jun 2011, AC 26 Apr 2012 and BG 26 Jul 2012, respectively.

Table 3 Mean flow and sediment parameters from spatially-averaged velocity profiles along dunes in the Paraná and Tercero rivers

Site and date	$u_*$ ( $m s^{-1}$ )	$k_s$ (m)	$r^2$	$\tau_0$ (Pa)	$\tau_*$	$Re_p$	$w_s$ ( $m s^{-1}$ )	$\tau_{*cs}$	$k_s/H_d$
TR 16 Mar 2016	0.117	0.16	0.95	13.59	0.43	346	0.195	1.30	0.40
TR 8 Apr 2016	0.127	0.34	0.99	16.18	0.51	346	0.195	1.30	0.71
TR 5 Sep 2016	0.059	0.09	0.91	3.49	0.11	346	0.195	1.30	0.45
TR 7 Nov 2016	0.084	0.14	0.94	7.00	0.22	346	0.195	1.30	0.58
Lavalle 2 Jun 2011	0.067	0.16	0.97	4.51	0.90	22	0.046	0.40	0.07
AC 26 Apr 2012	0.079	0.18	0.98	6.25	1.14	25	0.050	0.48	0.07
BG 26 Jul 2012	0.082	0.32	0.98	6.80	1.08	31	0.058	0.52	0.18

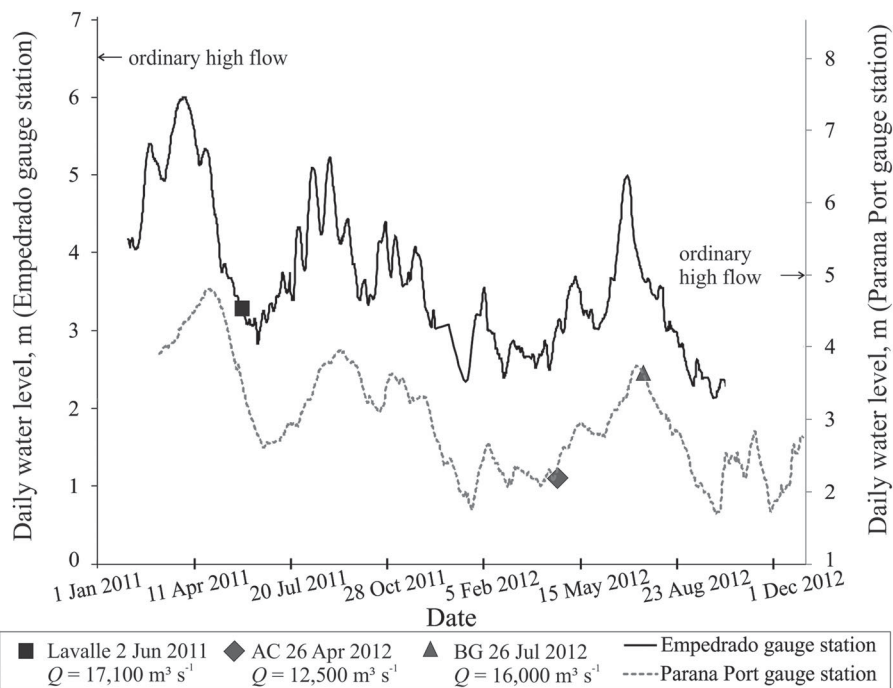


Figure 2 Hydrographs at two gauge stations (Empedrado and Paraná Port) in the Paraná River during 2011 and 2012. Dates of measurements at the three surveyed reaches (Table 2) are also included

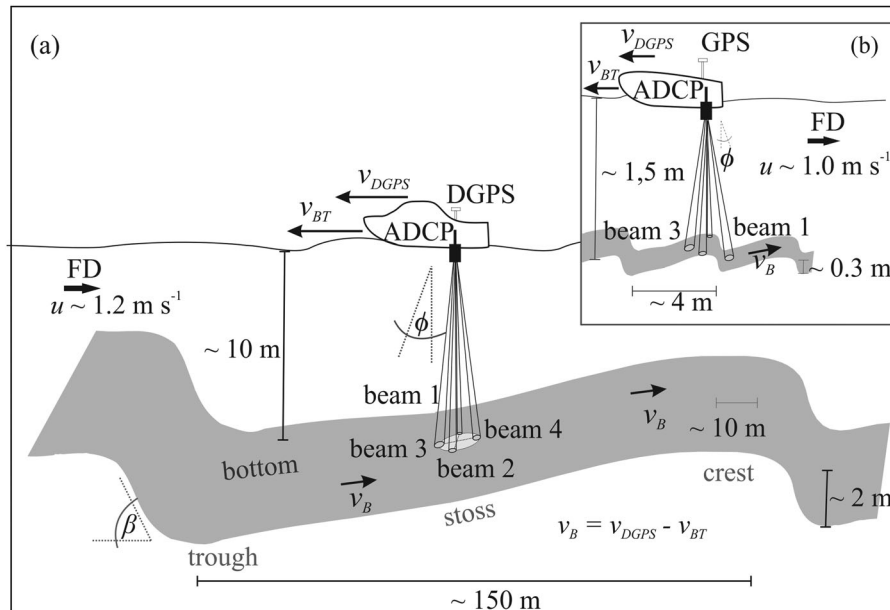


Figure 3 Schematics of ADCP beam alignments and corresponding footprints on the Paraná (a) and Tercero (b) dunes. Height and length scales of dunes are different in order to gain a better visualization. Footprints and dune length scales are nearly equal in order to obtain a representative size of the ensonified area due to beam spreading on the dune. (Adapted from Latosinski et al., 2017)

the flow configuration along it with a great detail. Estimations of the water surface slopes could also be obtained due to the high accuracy of the DGPS-RTK altitude data. In the Tercero River, dynamic measurements were performed along repeated longitudinal bathymetric profiles before and after the static measurements of ADCP to identify the surveyed dunes and define their geometric characteristics and dune celerity.

The ADCP static measurements were conducted over the selected dunes for each field site by anchoring the boat. Measurements involved time series of flow-velocity vertical profiles, echo intensity level, and bed-particle velocities over all selected dunes of both rivers. Moreover, due to the faster dune displacement observed in the Tercero River, the static measurements captured the passage of the whole study dune. The time intervals used in the static records were 2-3 h for the Tercero River and 15 min for the Paraná River. Along the studied dunes in the Paraná River, static measurements were performed at the crest, stoss-side and trough of each selected dune. The velocity of the particles moving within the bedload layer,  $v_B$ , was recorded during the static measurements at the crest, stoss and trough of each dune by means of the Bottom Track ADCP function (BT) according to the methodology presented by Latosinski et al. (2017). Figure 3 outlines the alignments of the four acoustic beams as projected from the ADCP and the corresponding footprint over the riverbed (dunes). It is worth noticing that the acoustic footprint defines the associated averaging area based on the beam divergence ( $\phi = 20^\circ$  or  $25^\circ$ , depending on the ADCP manufacturer, i.e. TRDI 1200 kHz or Sontek S5 ADCP, respectively) and flow depth. The  $v_B$  data in the Tercero River were obtained by selecting only those parts of the whole record over the dunes corresponding to the crest, stoss and trough sides. Due to the divergence of the ADCP beams close to the bed, data

of only one beam were considered in this case, i.e. beam 1 in Fig. 3b: the beam with a downstream horizontal component in a Janus or downward looking configuration (Simpson, 2001; Sonstek, 2013). Conversely, averages of the four beams' data were used in the Paraná River (Fig. 3) since it was assumed that divergence did not influence the results due to the large dune sizes (Latosinski et al., 2017).

The static measurements over different dune zones of the Paraná River were also useful to achieve suspended bed-sediment concentration (SSC) values from the acoustic records. The acoustic returns were processed following the ADCP-based acoustic inversion approach described in detail in Szupiany et al. (2019) using the ASET Matlab-toolbox (Dominguez Ruben et al., 2020).

### 3 Results

#### 3.1 Bedform geometry, mean flow, and sediment characteristics

Dune geometric features, sediment features, and flow parameters are shown in Table 2 to identify similarities and differences between these two alluvial rivers.

The Froude number ( $F_r$ ) is low for both streams, though higher in the Tercero River, 0.20-0.30 against 0.10-0.12 in the Paraná River. The relative dune heights,  $H_d/h$ , ranged from [0.16, 0.32] in the Tercero River to [0.16, 0.22] in the Paraná River. These  $H_d/h$  values are in the same range as those reported by Bradley and Venditti (2017) for dunes in sand bed rivers with low  $F_r$  ( $< 0.32$ ), and they are lower than values from laboratory experiments (Bradley & Venditti, 2019). Naqshband et al. (2014, table 1, fig. 1) reported similar findings, and Cisneros

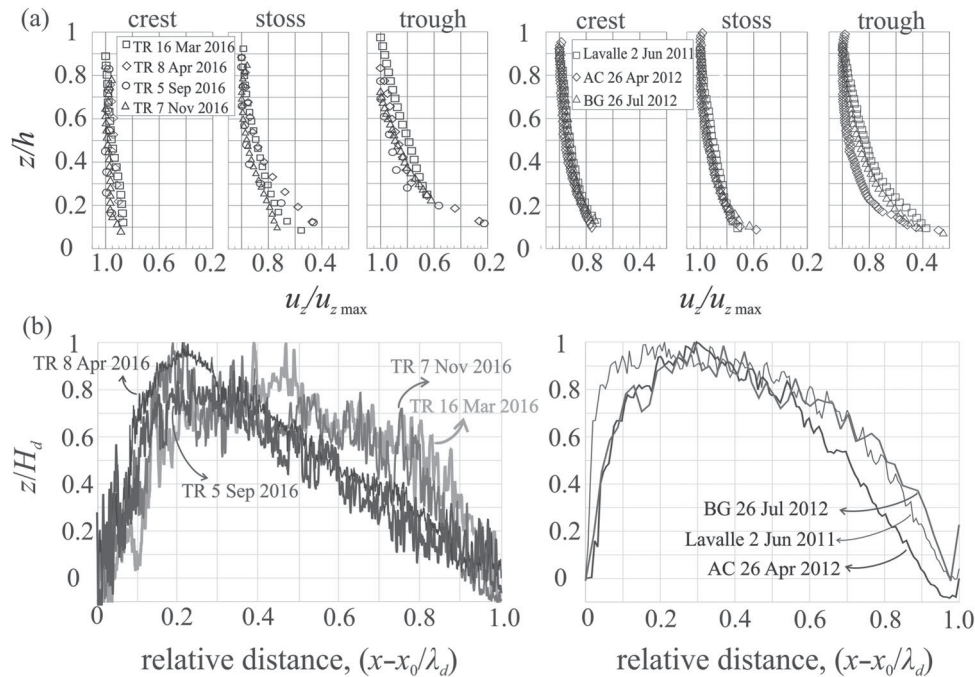


Figure 4 Dimensionless (a) flow velocity profiles at static measurements normalized with the maximum value within the water column, and (b) surveyed dune profiles from dynamic surveys, where the  $x_0$  progressive corresponded to the deepest bed level at the trough downstream of the crest of each dune. The values of  $u_{z\max}$  in  $\text{m s}^{-1}$  for crest, stoss and trough were 1.72, 1.68 and 1.24 (TR 16 Mar 2016), 1.44, 1.35 and 1.39 (TR 8 Apr 2016), 0.85, 0.79 and 0.78 (TR 5 Sep 2016), 0.82, 0.79 and 0.76 (TR 7 Nov 2016), 1.24, 1.16 and 1.16 (Lavalley 2 Jun 2011), 1.61, 1.54 and 1.48 (AC 26 Apr 2012), 1.37, and 1.31 and 1.22 (BG 26 Jul 2012)

et al. (2020) studied natural dunes with an even lower ratio, i.e.  $H_d/h < 0.1$ , than commonly assumed for large alluvial rivers.

Dimensionless dune profiles in both rivers were achieved by plotting the relative dune height ( $z/H_d$ ) versus the dimensionless or relative distance in upstream direction from the end of lee side to the dune trough (Fig. 4b and Table 2). All surveyed dunes collapse into a similar profile under the scaling of dune height and wavelength (Fig. 4b), within the bounds of the experimental errors. It seems that although the values of the form factor,  $\alpha$ , for the shape of the dunes for the Tercero River (average value,  $\alpha = 0.6$ ) resemble those of the Paraná River (average  $\alpha = 0.68$ ), they are closer to triangular-shaped dunes. Indeed, the triangular shape of the Tercero River dunes can be observed in Fig. 4b.

The steepness ( $H_d/\lambda_d$ ) values of the dunes in Tercero River have the same order of the ripple steepness ( $\approx 0.1$ ; Van Rijn, 1993) and are four to ten times larger than the steepness values of large dunes in the Paraná River, according to Table 2. Moreover, in the Paraná River, small superimposed dunes along the stoss side of large dunes were well defined by the longitudinal SBES records. These superimposed dunes present a mean length of 4.7, 5.4 and 8 m and a mean height of 0.19, 0.40 and 0.30 m for Lavalley 2 Jun 2011, AC 26 Apr 2012 and BG 26 Jul 2012, respectively. Further details of superimposed dunes in the Paraná River can be found in Latosinski et al. (2017). These dimensions perfectly fall into the range of values reported by Amsler and Schreider (1992) at another reach of the Paraná River. The steepness of small superimposed dunes is between

0.04 and 0.07 (Table 2), i.e. around two and seven times higher than the steepness of large dunes. In the Tercero River, superimposed dunes were not observed after visual inspection of the dune field. Note that the fluctuations observed in bed elevation in Fig. 4b resulted from Doppler noise rather than from real variations.

The lee-side angle,  $\beta$ , was obtained by calculating the slope of the bed tangential lines over each longitudinal profile. This allows obtaining the variation of the dune angle on its leeward side (Fig. 5). Regarding the upper zone of the lee side of the large dunes in the Paraná River, values were very low ( $\beta < 5^\circ$ , Fig. 5a), in the order of those reported by Amsler and Schreider (1992) for this type of dunes. The maximum angle occurs in the 10–30% lower portion of the lee side of Paraná dunes (Fig. 5a) reaching up to  $14^\circ$ ,  $15^\circ$  and  $5^\circ$  for Lavalley, Aguas Corrientes, and Bajada Grande, respectively. Meanwhile, in the Tercero River,  $\beta$  approaches the angle of repose ( $\sim 30^\circ$ ) practically over the entire lee side (Fig. 5b). Nonetheless, mean  $\beta$  values are presented, calculated as simple (and triangularly shaped) dune lee-sides joining the highest point at the crest with the deepest point at the trough (Table 2).

### 3.2 Flow pattern characterization

#### 3.2.1 Static measurements

Figure 4a represents, on top of the dimensionless dune profiles, the vertical distribution of the time-averaged flow velocity,  $\bar{u}_z$ ,

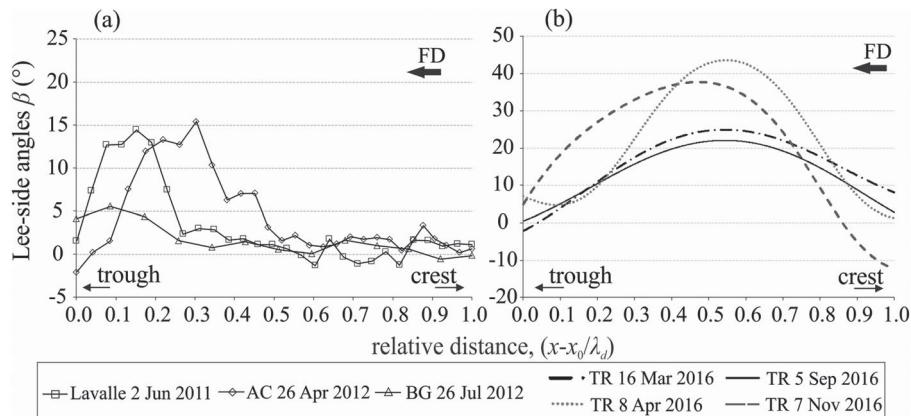


Figure 5 Lee side angle of dunes in the Paraná (a) and Tercero (b) Rivers. The  $x_0$  progressive corresponds to the deepest bed level at the trough downstream of the crest of the studied dunes, and the last progressive value corresponds to a vertical representative of the crest zone. Reported values are the slope (converted to degrees) of the lines joining the depth of successive ensembles at the lee-side. The origin of distances is close to the deepest point at the trough. Due to some dispersion for Tercero River data, raw depth values were treated with a band-pass filter. FD: flow direction

normalized with the maximum value within each profile,  $\bar{u}_z \max$ . The period for time-averaged values corresponded to the static measurement time intervals.

For each position on the dune, the overlapping of the velocity profiles from different lee dunes show some similarity for the same river (Fig. 4a). The largest discrepancies are observed in the trough areas. The flow velocity is of boundary layer type throughout the depth of the Paraná River, and more uniform in the water column of the Tercero River, particularly on the crest. It can be argued that the vorticity generated by the boundary resistance is spread across the water layer of the Paraná River. Meanwhile, it is likely that the vorticity generated on the crest of each Tercero River dune is confined to a thin boundary layer. These differentiated forms of vorticity diffusion can trigger different mechanisms of bed sediment transport.

In the Paraná River, the velocity profiles fit fairly well to the so-called “law of the wall” for turbulent boundary layers, in agreement with Trento et al. (1990). Moreover, these authors verified that the boundary layer on the dune crests reached 80–100% of the total flow depth. This fact can be explained by the gentle stoss side slopes of the dunes along the large wavelengths in the Paraná River (see  $\lambda_d$  values as reference in Table 2), which allow completion of the turbulent mixing. Conversely, the higher steepness values and shorter dune wavelengths in

the Tercero River would prevent complete development of the boundary layer.

The velocity profiles obtained with the ADCP from static measurements were used to estimate the total bed shear velocity,  $u_*$  (Table 4), applying the law of the wall (Holmes & García, 2008; Kostaschuk, Villard, & Best, 2004; Szupiany et al., 2007) in the manner suggested by Clauser (1956) and Blettlér et al. (2012), i.e. values of  $u_*$  determined from linear regressions of the form:

$$\bar{u}_z = a \log(z) + b \quad (1)$$

where  $\bar{u}_z$  is the time-averaged streamwise velocity at height  $z$  from the bed;  $a$  is the regression slope coefficient,  $a = 5.6u_*$ ; and  $b$  is the regression intercept coefficient which involves roughness height,  $b = u_*(8.15 - 5.6 \log k_s)$ .

The regression slopes for the velocity profiles in the dune troughs present high-velocity gradient and, therefore, higher shear stress values. However, the flow dynamics in the trough zone did not meet the conditions from which the semi-logarithmic expressions were derived (strong variations in the pressure gradient) and, therefore, were not considered in the analysis.

Semi-logarithmic regression of velocity profiles was typically observed at least in the lower 20–50% of total depth for

Table 4 Shear velocity  $\bar{u}_*$  ( $\text{m s}^{-1}$ ) and the corresponding  $r^2$  values at crest and stoss sides of dunes obtained by fitting Eq. (1) to the static time-averaged velocity profiles recorded in the Paraná and Tercero rivers

Site and date	Crest			Stoss			Average	
	$\bar{u}_*$	$r^2$	$(x_i/\lambda_d)$	$\bar{u}_*$	$r^2$	$(x_i/l_d)$	$\bar{u}_{*stoss}/\bar{u}_{*crest}$	$\bar{u}_{*stoss}/\bar{u}_{*crest}$
TR 16 Mar 2016	0.064	0.96	0.60	0.112	0.99	0.43	1.75	2.92
TR 8 Apr 2016	0.039	0.94	0.70	0.176	0.99	0.46	4.51	
TR 5 Sep 2016	0.040	0.76	0.79	0.090	0.96	0.52	2.25	
TR 11 Nov 2016	0.019	0.97	0.73	0.060	0.99	0.42	3.16	
Lavalle 2 Jun 2011	0.063	0.99	0.65	0.059	0.98	0.39	0.94	
AC 26 Apr 2012	0.106	0.99	0.55	0.098	0.99	0.45	0.92	
BG 26 Jul 2012	0.073	0.98	0.69	0.073	0.98	0.49	1.00	

both river crests and stoss. The relative position over the dune,  $x_i/\lambda_d$  (with  $x_i = 0$  being the position at the end of the lee-side) is shown in Table 4. The range from 20 to 50% of total depth used to fit velocity data may be somewhat arbitrary; however, deviations from semi-logarithmic regression were observed for the velocity profile data outside of that 20–50% range (principally at Tercero River), an issue extensively discussed in the literature (Kostaschuk et al., 2004; Trento et al., 1990; among others). Moreover, this range is successfully applied by Holmes and García (2008) to obtain local values of shear velocity of flow over dunes in the Missouri River.

Table 4 shows that in the Tercero River the shear velocities are, on average, three times higher on the stoss side than on the dune crests, while they show slow variations along the Paraná River dunes. Note that the effect of acoustic beam divergence and the small dune lengths in the Tercero River could account for such a difference. Therefore, mean velocity profiles and shear velocities were calculated over each dune, following the procedure detailed in the next section.

### 3.2.2 Longitudinal average velocities over the dune, computation of roughness and flow resistance

Figure 6 depicts the spatially-averaged velocity ( $u_z$ ) profiles over each selected dune obtained from the dynamic measurements in the Paraná River and the static continuous measurements in the Tercero River. Averages were carried out along lines at the same relative depth (dividing the water column into nine cells) from an initial boundary. The verification of a nearly constant specific discharge,  $\bar{q}$ , using the static measurements is achieved on the crest, stoss side and trough of all dunes. The differences in  $\bar{q}$  along the dune profiles in the Tercero River, although they could be considered important, were generally lower than 20%. In this case, as seen from static measurements for flow velocity on dune crests, measurement errors due to the effect of acoustic beams divergence and the small dune lengths could be responsible for the discrepancies.

The spatial averaging of velocity profiles in the Paraná River displays slightly better fits (Fig. 6). Main differences appear with the point data near the bottom, due to the larger scatter in the Tercero River. The greater relative length of the separation region (length of separation region/dune length) of dunes in the Tercero River, together with effects of beam divergence near the bed, could account for the observed deviation.

The fairly good fit of velocity profiles shown in Fig. 6 allows computation of the mean shear velocity ( $u_*$ ) and the equivalent roughness height ( $k_s$ ) by means of Eq. (1) (Table 3). Mean bed shear stress ( $\tau_0$ ), the Shields parameter ( $\tau_*$ ), and the Reynolds particle number ( $R_{ep}$ ) at the dunes can also be obtained by using the following equations:

$$\tau_0 = \rho u_*^2 \tag{2}$$

$$\tau_* = \frac{u_*^2}{sgD_{50}} \tag{3}$$

$$R_{ep} = \sqrt{sgD_{50}}D_{50}/\nu \tag{4}$$

where  $s = (\rho_s/\rho) - 1$  is the submerged specific gravity of sediment,  $\rho_s$  and  $\rho$  are sediment and water density, respectively,  $g$  is the gravitational constant,  $\nu$  is the kinematic viscosity, and  $u$  and  $h$  are the spatial averages of flow velocity and depth, respectively, at the selected dune (Table 2).

Table 3 shows the mean values of flow and sediment parameters along the dunes, deduced from the spatially-averaged velocity profiles, and the critical value of Shields parameter to convey sediments in suspension,  $\tau_{*cs}$ , following the Shields–Parker criteria (García, 2008).

According to the results in Table 3, the roughness values,  $k_s$ , are comparable to the dune height in the Tercero River and the mean height of the small superimposed dunes in the Paraná, i.e. between 0.20 and 0.40 m (Latosinski et al., 2017), as was anticipated by Amsler and Schreider (1992). The difference strengthens the hypothesis that the resistance in large rivers (like the Paraná) is governed by the small dunes superimposed

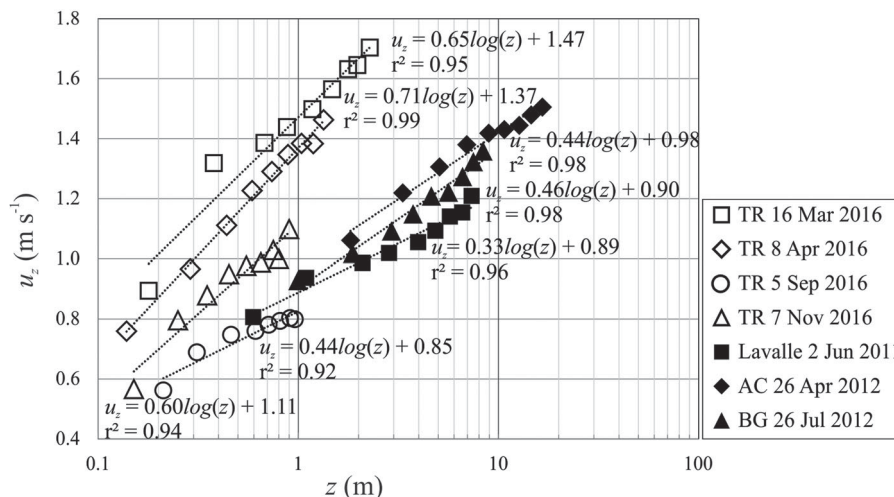


Figure 6 Velocity profiles spatially averaged on the studied dunes

to the larger ones as it was first proposed by Ogink (1989). Since the wavelength of the large dunes is many times larger than the mean flow depth, their effect on the mean flow conditions at the scale of the smaller dunes can be expected to be negligible. This topic is further discussed below in connection with bed sediment transport.

The normal flow approximation provides a quick insight into the role bedforms or sediment particles may play in the characteristic roughness height and the mode of sediment transport that occurs in the stream. The streamwise momentum balance equation, under the assumption of a very wide channel where the roughness of the banks is negligible, takes the form:

$$0 = -ghS + C_F u^2 \tag{5}$$

which yields the well-known relation  $F_r^2 = u^2/gh = S/C_F$ , i.e. the Froude number based on the normal flow quantities that result when friction and gravity are in perfect balance (while an increase in  $S$  tends to accelerate the flow, an increase in  $C_F$  has the opposite effect) (Vionnet, Tassi, & Martin-Vide, 2004). Here  $S$  is the friction slope, and  $C_F$  the bed resistance coefficient.

The second term of the Eq. (5) links the bed shear stress with the squared of the mean flow velocity,  $\tau_0 = \rho C_F u^2$ , that defines the bulk shear velocity for a very wide channel, where the hydraulic radius can be approximated by the mean flow depth:

$$u_{*b} = \sqrt{ghS} \tag{6}$$

which is equivalent to the root square of Eq. (2) and yields:

$$\frac{u}{u_{*b}} = \frac{1}{\sqrt{C_F}} = C_Z \tag{7}$$

where  $C_Z$  is the dimensionless Chezy resistance coefficient, and together with  $C_F$ , is a function of the relative bed roughness  $C_F^{-1/2} \equiv C_Z = f(h/k_{sb})$ , where the equivalent roughness height can be estimated as:

$$k_{sb} = \begin{cases} n_k D_{50}, & 1 \leq n_k \leq 3 \\ f(\Delta_d), & \text{van Rijn(1993)} \end{cases}$$

Above,  $k_{sb}$  denotes a roughness height usually proportional to a characteristic sediment size in case of a flat bed, or a dimension

proportional to the dune height,  $\Delta_d$ , in presence of bedforms (Van Rijn, 1993). This is because if dunes are present, the form drag prevails over the grain roughness or skin friction. The easiest way to determine the required amount of hydraulic resistance to keep the balance between a given friction slope and flow discharge is through a fixed-point iteration or a direct computation (Vionnet et al., 2004). Tables 1 and 2 summarize the used values of  $S$  and unit discharge  $q$  ( $q = hu$ ), respectively:

$$C_F^{(i)} = \frac{1}{\left[\frac{1}{\kappa} \ln \frac{11h^{(i)}}{k_{sb}}\right]^2}, \quad h^{(i+1)} = \left(\frac{q^2 C_F^{(i)}}{gS}\right)^{1/3}, \quad i = 0, 1, 2, \dots \tag{8}$$

The hydraulic resistance computations using Eq. (8) are presented in Table 5, based on the hydraulic and dune characteristics in Table 2. Moreover, Fig. 7 depicts the Keulegan (1938) relation for the Tercero and Paraná rivers as computed by Eq. (8), together with Gilbert’s field and flume data (Gilbert & Murphy, 1914) that includes flat bed and bedforms (Brownlie, 1981; Wong & Parker, 2006). This simple analysis confirms that boundary resistance for the Paraná River depends on the smaller superimposed dunes height,  $h/k_{sb} = h/\Delta_{sd}$ , which is in agreement with Amsler and Schreider (1992). For the Tercero River, the relative roughness factor  $h/k_{sb}$  fits with the observed dunes size,  $h/\Delta_d$  (Table 5). The box plots of Fig. 8 show, under the bounds of the normal flow approximation and experimental errors, that the estimated theoretical range of values is well within the observed range of field data. There is little offset with respect to the mean values of  $S/C_F$  between the two box plots to expose the max, mean, and min of the experimental and the theoretical values. This is to be expected since the ratio  $S/C_F$  is equivalent to the square of the Froude number (Eq. 5).

The discrepancies between some values of  $k_s$  listed in Tables 3 and 5 have several sources. Table 3 contains values obtained after two averaging processes in a row, over the turbulence and along the dune length, ignoring possible effects due to the three dimensionality of the flow. Table 5 exhibits the average values along several dunes, assuming a constant friction slope among other simplifications. Despite these discrepancies, which are most likely caused by the approximations made by different methods, the boundary resistance values obtained with both methods are highly consistent. This result supports the fact that the equivalent roughness height is comparable to the dune

Table 5 Hydraulic resistance and roughness parameters for the normal flow computations

	$S/C_F$	$k_{sb}$ (m)	$h/k_{sb}$	$\Delta_d = H_d$ (m)	$\Delta_{sd}$ (m)	$C_F^{-1/2}, C_Z$	$Re_p$	$\tau_{*b}$
TR 16 Mar 2016	0.086	0.55	4.5	0.40	-	9.77	346	0.699
TR 8 Apr 2016	0.099	0.25	6.0	0.48	-	10.5	346	0.420
TR 5 Sep 2016	0.045	0.71	1.6	0.20	-	7.1	346	0.308
TR 7 Nov 2016	0.078	0.29	3.8	0.24	-	9.3	346	0.308
Lavalle 2 Jun 2011	0.013	0.16	53	1.93	0.19	15.9	22	0.851
AC 26 Apr 2012	0.010	0.63	28.8	2.86	0.40	14.4	25	1.622
BG 26 Jul 2012	0.015	0.11	89.5	1.78	0.30	17.2	31	0.731

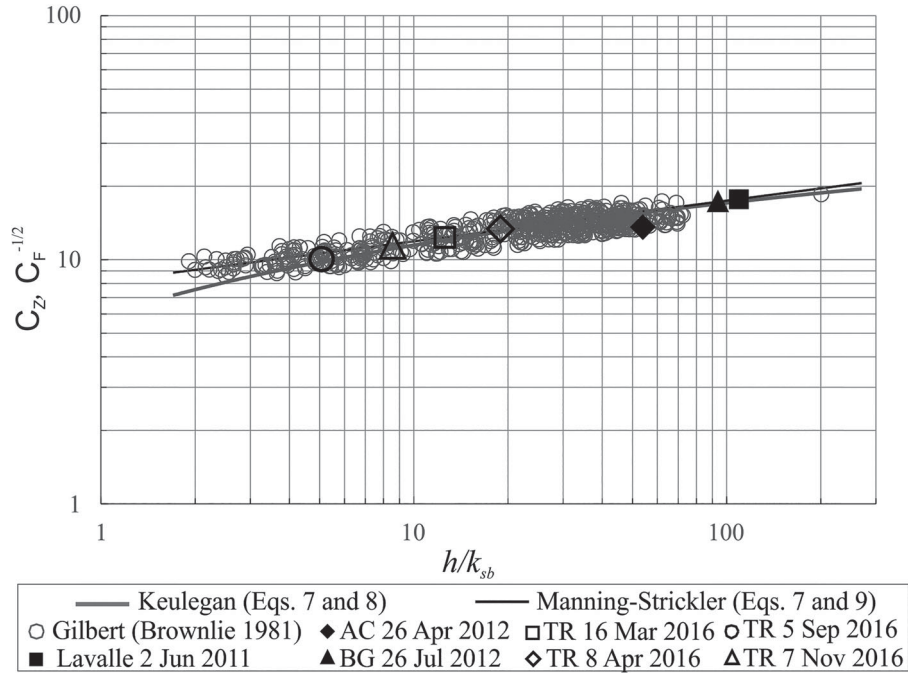


Figure 7 Resistance coefficients versus depth to roughness height ratio (relative roughness) for the laboratory dataset of Gilbert (Wong & Parker, 2006) plus the data for Paraná and Tercero rivers

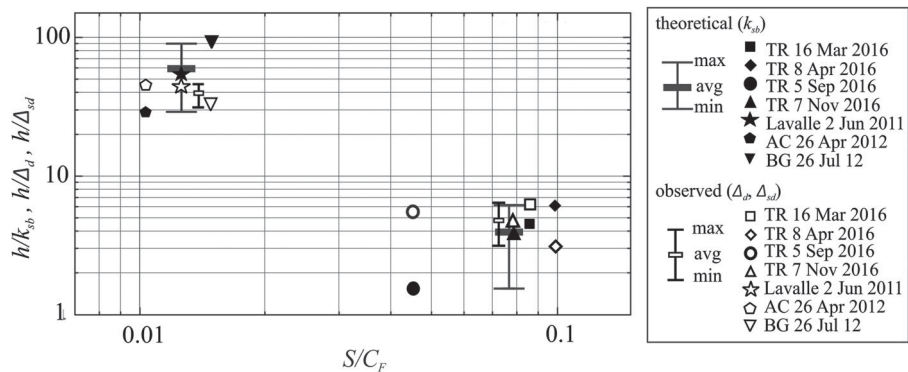


Figure 8 Dependence of the relative roughness factor with the square Froude number based on normal flow conditions ( $F_r^2 = S/C_F$ ). The fourth column of Table 5 is used for theoretical values at the ordinates, meanwhile fifth and sixth columns from the same table are used to compute the observed values

amplitude for the Tercero River and to the amplitude of the smaller superimposed dunes for the Paraná River.

Finally, Gioia and Bombardelli (2002) rederived the Manning-Strickler’s empirical formula (Eq. 9) from a power-law asymptotic behaviour of a channel flow of incomplete similarity in the relative roughness, whose fit to Keulegan’s resistance law was demonstrated by Wong and Parker (2006). It reads:

$$C_z = 8.10 \left( \frac{h}{k_{sb}} \right)^{1/6} \quad (9)$$

This relation is also included in Fig. 7, where the collapse between the Paraná and Tercero Rivers data with the field and lab data, collected by Brownlie, and used by Wong and Parker (2006), is found to be remarkably good.

Figure 7 shows that both rivers obey the same resistance law, either Keulegan (a wall-similarity law) or Manning–Strickler (a power-law asymptotic of incomplete similarity). However, when looking at the theoretical hydraulic resistance height of each river, and the value observed in the field (Fig. 8), it is seen that while the dunes of the Tercero River represent an effective roughness height, the Paraná River must develop an intermediate roughness scale, whose height is in tune with the heights of the small superimposed dunes. This is necessary to maintain the balance of forces between gravity and friction. Figure 7 represents a constitutive law, while Eq. (5) represents the true competition between forces, and to maintain it, the Paraná River must develop an intermediate roughness scale. Both resistance laws are well-grounded in turbulence theory through different techniques, one based on wall-similarity techniques and the other in a power-law asymptotic of incomplete similarity. The fit

between both analytic curves and the experimental data (Gilbert & Murphy, 1914) is remarkable.

### 3.3 Bed-sediment transport along dune profiles

Table 6 provides the magnitude values of bed-particle velocity,  $v_B$ , measured with the help of the ADCP technology along the dune profiles. Their magnitudes were comparable at both rivers, showing similar tendencies, i.e. increasing from troughs to crests (Latosinski et al., 2017). However, bedload rates,  $g_{sb}$  (computed with the dune tracking procedure and quartz specific weight,  $\gamma_s$ ), are somewhat higher for the Tercero River, at least regarding those two cases having higher flow discharge and shear velocity (i.e. the first two values for Site and date in Tables 2 and 6).

The fifth column of Table 6 presents the dune displacement velocity ( $u_d$ ) obtained from the comparisons of dynamic measurements applying the dune tracking method. As can be seen,  $u_d$  is considerably higher for the Tercero River than the Paraná River; however, the dune dimensions in the Tercero River are considerably smaller, finally yielding similar  $g_{sb}$  values.

The direction of  $v_B$  values is coincident with the mean flow direction in both the troughs and crests of the Paraná River dunes (Latosinski et al., 2017). This observation provides indirect evidence of the absence of recirculating flow at their troughs. Unfortunately, the directions for  $v_B$  measurements in the Tercero River were extremely noisy with wide variations, mostly at troughs. These variations could be ascribed, among other reasons, to the 3D structure of the recirculating flow at the troughs.

### 3.4 Suspended bed-sediment transport

The amount of suspended sediment differs significantly in both rivers. The Tercero River transports sediment predominantly as bedload, while the Paraná River conveys a large amount of sediment as washload (clay and silt) in suspension, as well as bed-material (fine and coarse sand) both in suspension and as

bedload. The absence of suspended bed particles in the Tercero River has to do with the larger grain sizes found in its bed, in comparison with the medium-sized sands found along the Paraná River bed. Figure 9 shows that the sediment particles of the Tercero River are transported as bedload since the stream-flow velocity exceeds the well-established threshold  $\tau_* > \tau_{*c}$  (Shields–Parker criteria, where  $\tau_{*c}$  is the critical value of motion for the Shields parameter; García, 2008) albeit being lower than the second threshold value of  $u_* / w_s \approx 1$  for the material to be transported in suspension. The results, extracted from Tables 3 and 5, coincide with both the normal flow approximation and the local-transient flow computation. As regards the Paraná River, the Shields parameter exceeds the predictive second threshold since the suspension number  $u_* / w_s > 1$  for all the observed values. Here,  $w_s$  is the settling velocity corresponding to the median diameter,  $D_{50}$ , of bed particles distribution, following van Rijn (1984).

The profiles of suspended bed sediment concentration over a dune in the Paraná River were obtained by processing the ADCP acoustic signal from static measurements, applying the methodology described in Szupiany et al. (2019) and Dominguez Ruben et al. (2020). The vertical distribution of suspended bed-sediment concentrations follows the typical Rouse shaped profile for bed-sediment particles conveyed in suspension. The concentration profiles can be converted to suspended bed-sediment transport profiles at crests, stoss sides and troughs of the surveyed dunes to obtain the suspended bed sediment loads ( $g_{ss}$ ). Such loads ( $g_{ss}$ ) at crests, stoss sides, and troughs of the surveyed dunes in the Paraná River as well as the ratio between  $g_{ss}$  at crest ( $g_{sscrest}$ ) and bed load transport rate ( $g_{sb}$ ) are presented in Table 6. The  $g_{sscrest}$  values are in the same range of values reported by Kostaschuk et al. (2009) at one dune in the Paraná River using similar surrogate technology. Additionally, the ratio  $g_{sscrest}/g_{sb}$  is about 10, which is the same order of magnitude previously reported by other authors (Alarcón et al., 2003; Amsler et al., 1999; Amsler & Prendes, 2000).

The pioneer investigations by Fredsøe (1981, 1982) showed both theoretical and experimentally that the increase/decrease

Table 6 Bed-particle velocity,  $v_B$ , from static measurement over dunes, dune displacement velocity ( $u_d$ ), bedload rate ( $g_{sb}$ ) for all measured dunes and suspended bed-sediment transport rate ( $g_{ss}$ ) and  $g_{sscrest}/g_{sb}$  ratio for the Paraná River dunes

Site and date	$v_B$ crest (m s <sup>-1</sup> )	$v_B$ stoss (m s <sup>-1</sup> )	$v_B$ trough (m s <sup>-1</sup> )	$u_d$ (m day <sup>-1</sup> )	$g_{sb}$ (kg m <sup>-1</sup> s <sup>-1</sup> )	$g_{ss}$ (kg m <sup>-1</sup> s <sup>-1</sup> )			$g_{sscrest}/g_{sb}$
						Crest	Stoss	Trough	
TR 16 Mar 2016	0.170	0.162	0.050	103.7	0.44	-	-	-	-
TR 8 Apr 2016	0.426	0.123	0.060	77.8	0.33	-	-	-	-
TR 5 Sep 2016	0.045	0.009	0.009	25.9	0.06	-	-	-	-
TR 7 Nov 2016	0.047	-	0.040	34.6	0.11	-	-	-	-
Lavalle 2 Jun 2011	0.045*	0.027*	0.006*	2.8	0.09	0.35	0.34	0.41	2.98
AC 26 Apr 2012	0.124*	0.099*	0.050*	3.9	0.11	0.27	0.27	0.24	2.48
BG 26 Jul 2012	0.052*	0.036*	0.009*	2.6	0.06	0.67	0.65	0.65	8.63

Notes: (\*) Data from Latosinski et al. (2017).

Stoss value of  $v_B$  in TR 7 Nov 2016 was discarded because of high instrument noise.

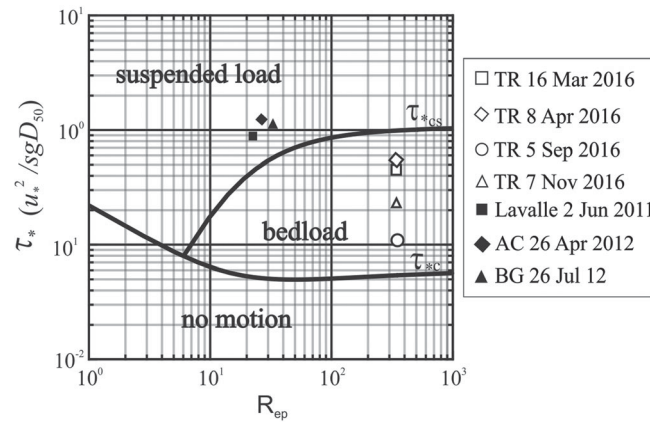


Figure 9 Shields–Parker (García, 2008) and Bagnold (1973) criteria for bedload and suspended-load thresholds. In the Paraná River, suspended transport dominates and in the Tercero River bedload transport prevails

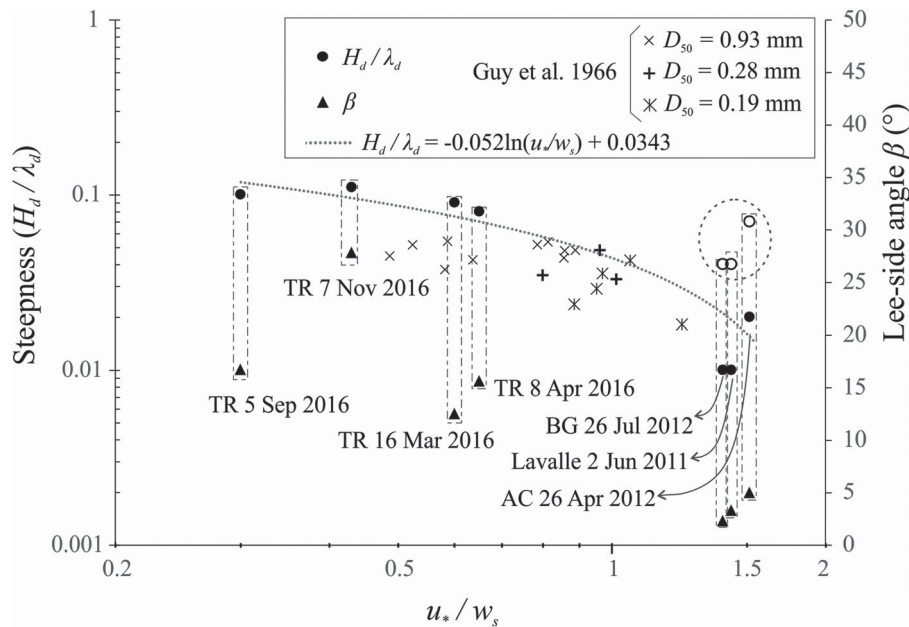


Figure 10 Relation between dune steepness ( $H_d/\lambda_d$ ) and mean lee side angle ( $\beta$ ) with the suspension number ( $u_*/w_s$ ) for the surveyed dunes in the Tercero and Paraná Rivers. Dune steepness from Guy et al. (1966) flume data for bed-sediment grain sizes of 0.19, 0.23 and 0.93 mm with different degrees of suspended bed-sediment transport, were also included. Dotted line: fit function for  $H_d/\lambda_d$  vs  $u_*/w_s$ . Encircled points: steepness of small superimposed dunes in the Paraná River (see Table 2)

in dune steepness depends on the suspended bed-sediment load/bedload transport ratio. If this ratio increases, steepness decreases and vice versa. Later on, and based on the Fredsøe’s approach, Amsler et al. (1999) explained the steepness variations of large dunes during floods in the Paraná River. Figure 10 summarizes the effects of increasing suspended bed loads (measured with the suspension number), on the morphology of the surveyed dunes in both rivers (steepness and lee-side angle). Data from Guy, Simons, and Richardson (1966) laboratory experiments are also included in Fig. 10. Note that despite the scatter due to the experimental error, the point data follow a diameter and steepness that decreases as the suspension number increases accompanied by the decrease in the mean lee-side angle.

#### 4 Discussion

The comparison of the dune morphology at different scales, flow structure, and prevailing sediment transport modes was carried out with data obtained in two alluvial rivers. Although the Paraná River dunes exhibited superimposed small dunes, reasonable dimensionless and similar profiles were achieved using the dune dimensions in both cases (Fig. 4b). The relative heights and form factor of dunes were in the same range for both rivers, as well as the  $F_r$  number, which is higher by a factor of three for the Tercero River. As expected, both rivers are in the subcritical flow regime (Chow, 1959). Steepness values were significantly smaller for the Paraná River,  $\sim 0.01$ - $0.02$ , than for the Tercero River,  $\sim 0.1$ . Another disparity was the maximum and

average value of the lee-side angles of dunes,  $\leq 15^\circ$  and  $5^\circ$ , for the Paraná River against  $\leq 38^\circ$  and  $29^\circ$  for the Tercero River, respectively.

Fairly good semi-logarithmic fits to velocity measurements enabled application of the “law of the wall” to obtain reliable values of bed shear velocities and stress in the Paraná River which increase, as expected, from the stoss side to the crest of dunes (Table 4 and Fig. 4a). It is likely that most of the vorticity is generated in the lee-side of the superimposed small dunes, and given the considerable extension of the large dunes, the boundary layer increases up to the surface (Fig. 4; Trento et al., 1990). In contrast, in the Tercero River, the boundary layer is limited to a small near-bed region showing velocity distributions that resembles potential flow profiles. The differences between shear velocity values on the stoss and the crest (ratios whose values goes from 1.8 to 4.5, Table 4) suggest that fitting parameters could not be representative of each zone of the dune. Beam divergence is a key factor when averaging data bouncing from very different zones of the Tercero River dunes. Moreover, the ADCP limitations to measure velocities in the 11–30% range of depth closest to the bed calls for the use of other methods to scan the Tercero River dunes (e.g. ADV/Flowtracker) for a detailed distribution of shear stresses along bedforms. When the velocity profiles are spatially averaged along the dunes (Table 3 and Fig. 6), notable improvements are obtained in the fitting parameters. Therefore, with these averages, good estimates of the bulk flow structure can be obtained in specific regions of the alluvial channel.

The main differences between both rivers could be attributed to the relative “smoothness”  $h/k_s$  factor. One order of magnitude separates the depth/roughness ratio of both rivers (Table 3 and Fig. 8). This could be explained in the Tercero River by the steepness and the lee-side angle  $\beta$ , which is  $\gg 11\text{--}20^\circ$  (Cisneros et al., 2020; Lefebvre, 2019; Lefebvre & Winter, 2016). The form drag of the large dunes in the Paraná River is negligible due to their shape, as first advanced by Ogink (1989) who performed careful laboratory experiments with dunes geometrically similar to bedforms measured in the Rhine River. These findings were later confirmed by Amsler and Schreider (1992) and Amsler and Prendes (2000) in the Paraná River. Therefore, the flow in the Paraná River seems less affected by the presence of large dunes, thus requiring a boundary resistance that scales with the roughness height of the superimposed small dunes, which are steeper (Table 2). It is possible to have a first quantitative idea of the extra roughness due to superimposition by using the results of the numerical experiments conducted by Lefebvre et al. (2016) based on flow and dune data similar to those measured at reaches of the upper Paraná and lower Rhine Rivers. They excluded the influence of superimposition and used a constant grain roughness of 3 mm. Their results of  $k_{sb}$  for lee angle dunes between  $7.5^\circ$  and  $20^\circ$  varied from 4.4 mm ( $7.5^\circ$ ) to 23 mm ( $20^\circ$ ), i.e. in the order of the grain roughness. When these values are compared to those obtained herein in the Paraná River (0.16–0.32 m; Table 3) with slip lee angles

between  $6^\circ$  and  $15^\circ$  (Fig. 5a), the influence of superimposition of dunes with comparable heights becomes relevant, accounting for the extra resistance (form resistance), necessary to balance the compelling forces.

The evidence that points to the absence of flow recirculation downstream of the crests of the large Paraná dunes arises from combining the angles of the lee side (Fig. 5a) with the velocity profiles averaged over time (Fig. 4a), and with the velocity of the bed particles at their troughs (Table 6). The most recent research works confirm that flow separation is likely to occur at the brink point, where the slope changes from being gentle to being steep at the lee-side (Cisneros et al., 2020; Lefebvre, 2019). Conversely, lee-side angles close to the angle of repose of sands for the Tercero River dunes (Fig. 5b) suggest flow separation downstream their crest. The directions of bed-particle velocity obtained from BT measurements support the above statement, although with limitations due to high noise levels of the Tercero River data.

The computed shear velocity values are similar for both rivers, although slightly higher for Tercero River. However, no bed-sediment suspension occurs in the Tercero River (Fig. 9) as a consequence of the higher mean grain size present at the bed and a low level of turbulence (Fig. 4a). In the Paraná River, the boundary resistance generates enough turbulence intensity (Fig. 4a) to keep bed sediment in suspension (Fig. 9). The decrease in dune steepness and lee-side angles with the relative predominance of suspended bed-sediment transport (Fig. 10) are in line with the pioneer results of Fredsøe (1982) and the findings of Bradley and Venditti (2017) and Bradley (2018 and references therein). Fredsøe (1981, 1982) firstly showed how increments of  $g_{ss}$  with respect to bed load,  $g_{sf}$ , as bed sediment sizes become smaller, lead to dunes with decreasing steepness, growing lengths and, finally, to the plane bed condition. Later on, several authors confirmed this role of  $g_{ss}$  on dunes through models and experiments of increasing complexities, though the internal mechanisms of the phenomenon are still a matter of debate (cf. Bradley, 2018; Bradley & Venditti, 2017; Naqshband et al., 2014). These facts would explain the absence of large dunes for high transport stages at a reach of the Paraná River (Amsler & García, 1997; Amsler et al., 1999) and the lowest lee-side angle and steepness of the BG 7/26/12 dune (Table 2). By plotting the  $H_d/\lambda$  and lee-angle values of all-natural dunes studied herein against the suspension number (Fig. 10), a collapse along a single relation shows the effect of relative bed-suspended loads on both geometric variables of dunes. When the flume data of Guy et al. (1966) are included in Fig. 10 to fill in the intermediate zone with  $H_d = 0.02\text{--}0.07$ , a fairly good relation is obtained. The results depicted in Fig. 10 confirm the trend exhibited by the descending branch of a cluster of field data plotted by Bradley and Venditti (2017). The steepness values of superimposed dunes in the Paraná River are included in the figure, and excluded from the relation. Their values (Table 2) differ more than 100% with respect to the values of large dunes (0.05 against 0.02 on average), suggesting

that suspension loads would only be important for large dunes (Amsler & García, 1997; Amsler & Schreider, 1992; Amsler & Prendes, 2000). Similar differences between steepness of both types of dunes are found in Julien (1992) and Ogink (1989). This allows appraisal of the above-mentioned effect on steepness on a quantitative basis. Then it is possible to argue that predominant suspended bed sediment loads could be a key factor governing the morphology of large dunes in low-gradient rivers in at least two geometric features: (i) the origin of the low lee-side angles; and (ii) the lower dune steepness as suspended bed sediment increases (e.g. Amsler et al., 1999; Bradley, 2018; Bradley & Venditti, 2017; Fredsøe, 1982; Kostaschuk et al., 2009; Kwoil et al., 2016; Schreider & Amsler, 1992; Tjerry & Fredsøe, 2005).

Finally, the different measurement sites of the Paraná River were selected by looking for a minimum impact of 3D effects of the channel morphology. However, it is well known that as the channel width increases so does the possibility of three-dimensional effects. Thus, the incidence of this factor would be inevitable in a wide channel such as the Paraná River, and could have affected the measurements. For instance, the different rates found in the suspended bed-sediment transport at each site in the Parana River could be due, in part, to the presence of 3D dunes in one site and 2D in another site. For the former, the transport rate could be lower, according to Parsons et al. (2005), and the flow separation zone should also be lower. This 3D effect was not assessed in the field measurements. However, for the purposes of this research, the 3D morphology does not affect the general results: looking at Fig. 10, the 3D effect could modify the position of the corresponding Paraná River values, in the context of high suspended sediments with very low steepness, with very low steepness approximately ten times smaller than Tercero River steepness.

## 5 Concluding remarks

In this work, several flow and bed sediment transport configurations over natural dunes of very different geometry (i.e. heights, lengths, lee-side angles) have been studied and compared based on data measured with high resolution, spatially as well as temporally, by using modern equipment (ADCP, GPS, DGPS-RTK and SBES). Measurements were performed at two sand bed rivers: the Paraná River (one of the largest in the world) and the Tercero River, a small tributary from the central region of Argentina.

It was possible to obtain similar velocity distributions on different positions along a similar dimensionless dune profile using proper scaling. The dune troughs exhibit major discrepancies. The flow velocity profile has the aspect of a fully developed boundary layer in the Paraná River, while it shows a potential flow type for the Tercero River, particularly on the crest. While the vorticity generated by form resistance is spread throughout the water depth of the Paraná River, it is confined to a thin

boundary layer for the Tercero River. Main differences between both rivers are:

- (a) particle number (larger in the Tercero River);
- (b) dune steepness (higher in the Tercero River if compared to the large and even the small superimposed dunes in the Paraná River);
- (c) lee-side angles of dunes (very low lee angles which would prevent permanent flow separation in the Paraná River compared to the lee angles of dunes in the Tercero River);
- (d) the superimposition of dunes in the Paraná River (small dunes on large dunes; absent in the Tercero River);
- (e) the “smoothness” factor,  $h/k_s$  (while the roughness height scales with the dune size for the Tercero River, in the case of the Paraná River it scales with the superimposed small dunes); and
- (f) the bed sediment transport mode (only bed load in the Tercero River and prevailing suspended loads in the Paraná River).

The differences stated above have at least two implications. While both are known by river researchers, few investigations have focused on detailed measurements along natural dunes, and particularly, along natural dunes in one of the largest rivers of the world.

- (i) The bulk of the form drag in the Paraná River would be carried by the small superimposed dunes since flow separation on the lee side of large dunes would be meaningless, eventually intermittent and likely affected 3D effects of dunes. This “smoothness” factor would explain its lower flow resistance with respect to the Tercero River. Somehow, the Paraná River develops an intermediate roughness scale between the grain size and the height of the large dunes to maintain the balance between the compelling mechanisms of gravity and friction, as reflected by Eq. (5). The field data of both rivers not only obey Keulegan’s resistance law but also represent different hydraulic resistance scales.
- (ii) The increase of bed suspended loads,  $g_{ss}$ , is closely associated with lower dune steepness and lee side angles of large dunes. Thus, suspension would be the link between the geometry of large dunes and their lesser role in the resistance to flow in the Paraná River.

The suspension number (or Bagnold’s number),  $u_* / w_s$ , used by many authors (e.g. Bradley, 2018), is an adequate parameter to account for the amount of suspended load and as such would be related to variations of dune steepness and lee-side angles. Indeed, the values of  $H_d / \lambda_d$  of dunes and large dunes measured in the Tercero and Paraná Rivers, respectively, together with steepness values of laboratory dunes, collapse along a single

relation when plotted against  $u_*/w_s$  (Fig. 10). The lee angle  $\beta$  follows a similar tendency.

It can be concluded that the suspension number is a key metric which helps to explain the differences in the geometry of alluvial dunes within a wide range of flow conditions. To determine the interactions of suspended particles near the bottom with the low lee-side angles of large dunes in big rivers, further investigations should be conducted combining mathematical modelling with field measurements like those presented herein. Note, also, that if dune superimposition is present as in very large rivers (Cisneros et al., 2020), the steepness of the smaller superimposed dunes (two to seven times greater than the steepness of the large dunes) does not fit the relation in Fig. 10, thus suggesting that the geometry of these dunes is driven mainly by mechanisms other than those related to particle suspension. Moreover, the superimposition of dunes at the bottom of many large rivers remains an open field of research.

### Acknowledgements

The authors gratefully appreciate the efforts of Cristian Vera and Santiago Cañete from the Faculty of Engineering and Water Sciences of the Universidad Nacional del Litoral who collaborated tirelessly in the Paraná River fieldworks. The authors also acknowledge the logistic support for conducting measurements in the Tercero River provided by the Provincial Administration of Water Resources (APRHi) of Córdoba administration. The support of the M.T. Geoffrey Yeh Chair in Civil Engineering at the University of Illinois at Urbana-Champaign is gratefully acknowledged. The authors are deeply grateful to two anonymous reviewers whose comments and suggestions undoubtedly improved the first draft of the manuscript.

### Disclosure statement

No potential conflict of interest was reported by the authors.

### Funding

The investigation was funded by the Faculty of Engineering and Water Sciences of the Universidad Nacional del Litoral (CAID 2016: “Bifurcations in the Paraná River system: hydro-sedimentological processes and implications in its morphodynamics” (in Spanish) and “Interdisciplinary evaluation of processes for the opening, maintenance and closure of secondary channels of the Paraná River” (in Spanish)).

### Notation

$a$  = slope of the linear regression of semi-logarithmic velocity profiles ( $\text{m s}^{-1}$ )

$b$	= regression intercept coefficient of semi-logarithmic velocity profiles ( $\text{m s}^{-1}$ )
$B$	= mean cross-section width (m)
$C_F$	= standard friction coefficient (–)
$C_Z$	= dimensionless Chezy resistance coefficient (–)
$D_{50}$	= mean grain size of bed material (m)
$F_r$	= Froude number (–)
$g_{sb}$	= unit bedload rate ( $\text{kg s}^{-1} \text{m}^{-1}$ )
$G_{sb}$	= total bedload transport at the cross-section ( $\text{kg s}^{-1}$ )
$g$	= gravitational constant ( $\text{m s}^{-2}$ )
$g_{ss}$	= suspended bed-sediment transport rate per unit width ( $\text{kg s}^{-1} \text{m}^{-1}$ )
$g_{sscrest}$	= unit suspended bed-sediment transport estimated from static measurements over the dune crest ( $\text{kg s}^{-1} \text{m}^{-1}$ )
$G_{ss}$	= total suspended bed-sediment transport at the cross-section ( $\text{kg s}^{-1}$ )
$G_w$	= total washload at the cross-section ( $\text{kg s}^{-1}$ )
$h$	= mean water depth (m)
$H_d$	= dune height (m)
$k_s$	= equivalent total roughness height (m)
$k_{sb}$	= roughness height from normal flow approach (m)
$Q$	= flow discharge ( $\text{m}^3 \text{s}^{-1}$ )
$q$	= unit flow discharge ( $\text{m}^2 \text{s}^{-1}$ )
$\bar{q}$	= time averaged unit flow discharge ( $\text{m}^2 \text{s}^{-1}$ )
$\text{Re}_p$	= Reynolds particle number (–)
$S$	= hydraulic gradient (assumed as general water surface gradient) (–)
$s$	= submerged specific gravity of sediment (–)
$u$	= mean flow velocity ( $\text{m s}^{-1}$ )
$u_d$	= dune celerity ( $\text{m d}^{-1}$ )
$u_z$	= spatially averaged velocity (over a dune) at level $z$ ( $\text{m s}^{-1}$ )
$\bar{u}_z$	= mean flow velocity (temporal averaged) at level $z$ ( $\text{m s}^{-1}$ )
$u_*$	= shear velocity ( $\text{m s}^{-1}$ )
$u_{*b}$	= bulk shear velocity ( $\text{m s}^{-1}$ )
$\bar{u}_*$	= shear velocity from static velocity profile (temporal averaging) ( $\text{m s}^{-1}$ )
$v_B$	= bed-particle velocity ( $\text{m s}^{-1}$ )
$w_s$	= settling velocity ( $\text{m s}^{-1}$ )
$z$	= level, height from the bed (m)
$\alpha$	= dune form factor (–)
$\beta$	= lee-side angle of the dune ( $^\circ$ )
$\gamma_s$	= quartz specific weight, ( $\text{kg m}^{-3}$ )
$\lambda_d$	= dune length (m)
$\kappa$	= von Kármán constant (–)
$\phi$	= ADCP transducer pointing angle from the vertical ( $^\circ$ )
$\rho$	= water density, $\text{kg m}^{-3}$
$\rho_s$	= bed sediment density, $\text{kg m}^{-3}$
$\nu$	= kinematic viscosity of water ( $\text{m}^2 \text{s}^{-1}$ )
$\sigma_g$	= geometric deviation of grain size distribution (–)
$\tau_0$	= total shear stress acting at the bed (Pa)

- $\tau_*$  = Shields number, or dimensionless shear stress (–)  
 $\tau_{*c}$  = threshold Shields number for initiation of motion (–)  
 $\tau_{*cs}$  = threshold Shields number for suspension (–)

## ORCID

Marcelo H. García  <http://orcid.org/0000-0003-0643-489X>

## References

- Alarcón, J., Szupiany, R., Montagnini, M., Gaudin, H., Prendes, H., & Amsler, M. (2003, de Noviembre 12–14). Evaluación del transporte de sedimentos en el tramo medio del río Paraná. *Proc., Primer Simposio Regional sobre Hidráulica de Ríos*, INA, Bs. As., Argentina.
- Amsler, M. L., & García, M. H. (1997). Discussion of: Sand-Dune Geometry of large rivers during floods by PY Julien & GJ Klaasen. *Journal of Hydraulic Engineering, ASCE*, 123(6), 582–585. doi:10.1061/(ASCE)0733-9429(1997)123:6(582)
- Amsler, M. L., & Prendes, H. H. (2000). Transporte de Sedimentos y Procesos Fluviales Asociados (233-306). In C. Paoli, & M. Schreider (Eds.), *El Río Paraná en su Tramo Medio. Tomo 1* (312 p.). Centro de Publicaciones. Universidad Nacional del Litoral. Santa Fe. Argentina. (In Spanish).
- Amsler, M. L., & Schreider, M. I. (1992, de Septiembre 8–12). Aspectos hidráulicos de la superposición de formas de fondo en el río Paraná (Argentina). *Memorias XV Congreso Latinoamericano de Hidráulica. Vol. 3*. Cartagena. Colombia.
- Amsler, M. L. & Schreider, M. I. (1999), Dunes Height Prediction at Floods in the Paraná River (Argentina). In: A. Jayawardena, J. Lee, & Z. Wang (Eds) *River Sedimentation – Theory and Applications* (pp. 615–620). Proceedings of the Seventh International Symposium on River Sedimentation (Hong Kong: 16-18/12/1998). A. A. Balkema.
- Bagnold, R. A. (1973). The nature of saltation and bed-load transport in water. *Proceedings of the Royal Society of London. A. Mathematical and Physical Sciences*, 332(1591), 473–504. doi:10.1098/rspa.1973.0038
- Best, J. (2005). The fluid dynamics of river dunes: A review and some future research directions. *Journal of Geophysical Research: Earth Surface*, 110, F04S02.
- Blettler, M., Amsler, M. & Ezcurra De Drago, I. (2012). Hydraulic factors controlling the benthic invertebrate distribution within and among dunes of the Middle Paraná River (Argentina) and sampling techniques. *Journal of South American Earth Sciences*, 35(2012), 27–37. doi:10.1016/j.jsames.2011.11.003
- Bradley, R. W. (2018). Controls on Dune Dimensions in Rivers, Thesis Submitted in Partial Fulfillment of the Requirements for the Degree of Doctor of Philosophy, Department of Geography, Faculty of Environment, Simon Fraser University.
- Bradley, R. W., & Venditti, J. G. (2017). Reevaluating dune scaling relations. *Earth-Science Reviews*, 165, 356–376. doi:10.1016/j.earscirev.2016.11.004
- Bradley, R. W., & Venditti, J. G. (2019). Transport Scaling of Dune Dimensions in Shallow Flows. *Journal of Geophysical Research: Earth Surface*, 124(2), 526–547. doi:10.1029/2018JF004832
- Brownlie, W. R. (1981). Compilation of alluvial channel data: laboratory and field, Report No. KH-R~43B, W. M. Keck Laboratory of Hydraulics and Water Resources, Division of Engineering and Applied Science, California Institute of Technology, Pasadena, California.
- Chow, V. T. (1959). *Open Channel Hydraulics*. McGraw-Hill.
- Cisneros, J., Best, J., van Dijk, T., de Almeida, R. P., Amsler, M., Boldt, J., Freitas, B., Galeazzi, C., Huizinga, R., Ianniruberto, M., Ma, H., Nittrouer, J., Oberg, K., Orfeo, O., Parsons, D., Szupiany, R., Wang, P., & Zhang, Y. (2020). Dunes in the world's big rivers are characterized by low-angle lee-side slopes and a complex shape. *Nature Geoscience*, 13(2), 156–162. doi:10.1038/s41561-019-0511-7
- Clauser, F. H. (1956). The turbulent Boundary Layer. *Advances in Applied Mechanics*. 4, 1–51.
- Dominguez Ruben, L., Szupiany, R., Latosinski, F., López Weibel, C., Wood, M., & Boldt, J. (2020). Acoustic Sediment Estimation Toolbox (ASET): A software package for calibrating and processing TRDI ADCP data to compute 2 suspended-sediment transport in sandy rivers. *Computers & Geosciences*, 140, 104499. doi:10.1016/j.cageo.2020.104499
- Fredsøe, J. (1981). Unsteady flow in straight alluvial streams. Part 2. Transition from dunes to plane bed. *Journal of Fluid Mechanics*, 102, 431–453. doi:10.1017/S0022112081002723
- Fredsøe, J. (1982). Shape and dimensions of stationary dunes in rivers. *Journal of the Hydraulics Division. ASCE*, 108(8), 932–947. doi:10.1061/JYCEAJ.0005896
- García, M. H. (2008). Sediment transport and morphodynamics (21–163). In M. H. García (Ed.), *Sedimentation Engineering: Processes, Management, Modeling, and Practice. ASCE Manuals and Reports on Engineering Practice No. 110: 1103 p.* ASCE.
- Gilbert, G. K., & Murphy, E. C. (1914). *The transportation of Debris by running water, professional paper 86, U.S. Geological Survey*. Report: 263 p.; 3 Plates. doi:10.3133/pp86
- Gioia, G., & Bombardelli, F. A. (2002). Scaling and Similarity in Rough Channel Flows. *Physical Review Letters*, 88(20), 1. doi:10.1103/PhysRevLett.88.204302
- Guy, H. P., Simons, D. B., & Richardson, E. V. (1966). Summary of alluvial channel data from flume experiments, 1956-61, Sediment transport in alluvial channels, Geological Survey professional paper 462-1, Washington D.C., USA.
- Herrero, H. S., Díaz Lozada, J. M., García, C. M., Szupiany, R. N., Best, J., & Pagot, M. (2018). The influence of tributary flow density differences on the hydrodynamic

- behavior of a confluent meander bend and implications for flow mixing. *Geomorphology*, 304, 99–112. doi:10.1016/j.geomorph.2017.12.025
- Holmes, R. R., & García, M. H. (2008). Flow over bedforms in a large sand-bed river: A field investigation. *Journal of Hydraulic Research*, 46(3), 322–333. doi:10.3826/jhr.2008.3040
- Julien, P. Y. (1992). *Study of bedform geometry in large rivers*. Delft Hydraulics - Colorado State University. Report Q 1386, Delft, The Netherlands.
- Kennedy, J. F. (1975). Hydraulic relations for alluvial streams. In V. A. Vanoni (Ed.), *Sedimentation Engineering (Chapter II: 114-154)*. ASCE - Manuals and Reports on Engineering Practice - No. 54. N. York. 745 p.
- Keulegan, G. H. (1938). Laws of turbulent flows in open channels. *Journal of Research of the National Bureau of Standards*, 21(6), 707–741. doi:10.6028/jres.021.039
- Kostachuk, R. (2000). A field study of turbulence and sediment dynamics over subaqueous dunes with flow separation. *Sedimentology*, 47(3), 519–531. doi:10.1046/j.1365-3091.2000.00303.x
- Kostaschuk, R., Shugar, D., Best, J., Parsons, D., Lane, S., Hardy, R., & Orfeo, O. (2009). Suspended sediment transport and deposition over a dune: Río Paraná, Argentina. *Earth Surface Process and Landforms*, 34(12), 1605–1611. doi:10.1002/esp.1847
- Kostaschuk, R., Villard, P., & Best, J. (2004). Measuring velocity and shear stress over dunes with acoustic Doppler profiler. *Journal of Hydraulic Engineering*, 130(9), 932–936. doi:10.1061/(ASCE)0733-9429(2004)130:9(932)
- Kwoll, E., Venditti, J. G., Bradley, R. W., & Winter, C. (2016). Flow structure and resistance over subaqueous high- and low-angle dunes. *Journal of Geophysical Research: Earth Surface*, 121(3), 545–564. doi:10.1002/2015JF003637
- Latosinski, F. G., Szupiany, R. N., Guerrero, M., Amsler, M. L., & Vionnet, C. (2017). The ADCP's bottom track capability for bedload prediction: Evidence on method reliability from sandy river applications. *Flow Measurement and Instrumentation*, 54, 124–135. doi:10.1016/j.flowmeasinst.2017.01.005
- Lefebvre, A. (2019). Three-dimensional flow above river bedforms: Insights from numerical modeling of a natural dune field (Río Paraná, Argentina). *Journal of Geophysical Research: Earth Surface*, 124(8), 2241–2264. doi:10.1029/2018JF004928
- Lefebvre, A., Paarlberg, A. J., & Winter, C. (2016). Characterising natural bedform morphology and its influence on flow. *Geo-Marine Letters*, 36(5), 379–393. doi:10.1007/s00367-016-0455-5
- Lefebvre, A., & Winter, C. (2016). Predicting bed form roughness: the influence of lee side angle. *Geo-Marine Letters*, 36, 121–133. doi:10.1007/s00367-016-0436-8.
- McLean, S. R., Wolfe, S. R., & Nelson, J. M. (1999). Predicting boundary shear stress and sediment transport over bedforms. *Journal of Hydraulic Engineering*, 125(7), 725–736. doi:10.1061/(ASCE)0733-9429(1999)125:7(725)
- Myrow, P. M., Jerolmack, D., & Taylor PerronNelson, J. (2018). Bedform disequilibrium. *Journal of Sedimentary Research*, 88(9), 1096–1113. doi:10.2110/jsr.2018.55
- Naqshband, S., Ribberink, J. S., & Hulscher, S. J. M. H. (2014). Using both free surface effect and sediment transport mode parameters in defining the morphology of river dunes and their evolution to upper stage plane beds. *Journal of Hydraulic Engineering*, 140(6), 1–6. doi:10.1061/(ASCE)HY.1943-7900.0000873
- Nelson, J. M., McLean, S. R., & Wolfe, S. R. (1993). Mean Flow and Turbulence Fields Over Two-Dimensional Bed Forms. *Water Resources Research*, 29(12), 3935–3953. doi:10.1029/93WR01932
- Ogink, H. (1989). *Hydraulic roughness of single and compound bed forms. Part XI. Report on model investigations*. Delft Hydraulics Laboratory, Delft.
- Parsons, D. R., Best, J. L., Orfeo, O., Hardy, R. J., Kostashuk, R., & Lane, S. N. (2005). Morphology and flow fields of three-dimensional dunes, Río Paraná, Argentina: results from simultaneous multibeam echo sounding and acoustic Doppler current profiling. *Journal of Geophysical Research: Earth Surface*, 110(F4). doi:10.1029/2004JF000231.
- Riccardi, G., Basile, P., Zimmermann, E., Stenta, H., Bussi, P., Mangiameli, P., & Pesci, M. (2013). *Diseño de presas de navegación en el estudio de prefactibilidad para el aprovechamiento del río Carcarañá como vía fluvial navegable*, Sexto Simposio Regional sobre Hidráulica de Ríos, FICH-UNL, 6-8 de Noviembre, Santa Fe.
- Schmeeckle, M. W., Shimizu, Y., Hoshi, K., Baba, H., & Ikezaki, S. (1999, September 6–10). Turbulent structures and suspended sediment over two-dimensional dunes. *River, Coastal and Estuarine Morphodynamics, Proceedings, International Association for Hydraulic Research Symposium*, pp. 261–270, Springer, New York.
- Schreider, M. I., & Amsler, M. L. (1992). Bedforms steepness in alluvial streams. *Journal of Hydraulic Research*, 30(6), 725–743. doi:10.1080/00221689209498904
- Shugar, D. H., Kostachuk, R., Best, J. L., Parsons, D. R., Lane, S. N., Orfeo, O., & Hardy, R. J. (2010). On the relationship between flow and suspended sediment transport over the crest of a sand dune, Río Paraná, Argentina. *Sedimentology*, 57(1), 252–272. doi:10.1111/j.1365-3091.2009.01110.x
- Simons, D. B., Richardson, E. V., & Nordin, C. F., Jr (1965). Bedload equations for ripples and dunes. U.S. Geological Survey Professional Paper, 462-H.
- Simpson, M. R. (2001). *Discharge Measurements Using a Broad-Band Acoustic Doppler Current Profiler*. Open File Report 01-1, United States Geological Survey, Sacramento, California.
- Smith, J. D., & McLean, S. R. (1977). Spatially Averaged Flow Over a Wavy Surface. *Journal of Geophysical Research*, 82(12), 1735–1746. doi:10.1029/JC082i012p01735

- Sontek, Y. S. I. (2013). River Surveyor S5/M9 System Manual. San Diego.
- Szupiany, R., Lopez Weibel, C., Guerrero, M., Latosinski, F., Wood, M., Dominguez Ruben, L., & Oberg, K. (2019). Estimating sand concentrations using ADCP-based acoustic inversion in a large fluvial system characterized by bi-modal suspended-sediment distributions. *Earth Surface Processes and Landforms*, 44(6), 1295–1308. doi:[10.1002/esp.4572](https://doi.org/10.1002/esp.4572).
- Szupiany, R. N., Amsler, M. L., Best, J. L., & Parsons, D. R. (2007). Comparison of Fixed- and Moving Vessel Measurements with an ADP in a Large River. *Journal of Hydraulic Engineering*, 133(12), 1299–1309. doi:[10.1061/\(ASCE\)0733-9429\(2007\)133:12\(1299\)](https://doi.org/10.1061/(ASCE)0733-9429(2007)133:12(1299))
- Tjerry, S., & Fredsøe, J. (2005). Calculation of dune morphology. *Journal of Geophysical Research*, 110(F4), F04013. doi:[10.1029/2004JF000171](https://doi.org/10.1029/2004JF000171)
- Trento, A., Amsler, M. L., & Pujol, A. (1990). *Perfiles observados de velocidad en un tramo del río Paraná-Análisis teórico*, XIV Congreso Latinoamericano de Hidráulica, IAHR, Montevideo, Uruguay.
- Van Rijn, L. C. (1993). *Principles of sediment transport in river, estuaries and coastal seas*, Aqua Publications, Amsterdam, The Netherlands, Chapter 5-5.2, pp 5.1-5.22, Chapter 7-7.2, pp 7.2-7.97.
- Van Rijn, L. C. (1984). Sediment transport. Part I. Bed load transport. *Journal of Hydraulic Engineering*, 110(10), 1431–1456. doi:[10.1061/\(ASCE\)0733-9429\(1984\)110:10\(1431\)](https://doi.org/10.1061/(ASCE)0733-9429(1984)110:10(1431))
- Vionnet, C. A., Tassi, P., & Martin-Vide, J. (2004). Estimates of flow resistance and eddy viscosity coefficients for 2D modeling on vegetated floodplains. *Hydrological Processes*, 18(15), 2907–2926. doi:[10.1002/hyp.5596](https://doi.org/10.1002/hyp.5596)
- Wong, M., & Parker, G. (2006). Reanalysis and correction of bed-load relation of Meyer-Peter and Müller using their own database. *Journal of Hydraulic Engineering*, 132(11), 1159–1168. doi:[10.1061/\(asce\)0733-9429\(2006\)132:11\(1159\)](https://doi.org/10.1061/(asce)0733-9429(2006)132:11(1159))
- Yalin, M. S., & Karahan, E. (1979). Steepness of Sedimentary Dunes. *Journal of the Hydraulics Division, ASCE*, 105(HY4), 381–392. April. doi:[10.1061/JYCEAJ.0005179](https://doi.org/10.1061/JYCEAJ.0005179)